Time-Dependent Gel to Gel Transformation of a Peptide based Supramolecular Gelator

Article *in* Soft Matter · May 2015

DOI: 10.1039/C5SM00808E

CITATIONS
54

READS
652

6 authors, including:

Arindam Banerjee
Indian Association for the Cultivation of Science
166 PUBLICATIONS **7,045** CITATIONS
SEE PROFILE

Abhishek Baral
University of Strasbourg
14 PUBLICATIONS **733** CITATIONS
SEE PROFILE

Shibaji Basak
Università degli Studi di Trento
21 PUBLICATIONS **1,016** CITATIONS
SEE PROFILE

Kingshuk Basu
Hebrew University of Jerusalem
21 PUBLICATIONS **445** CITATIONS
SEE PROFILE

Soft Matter

PAPER

View Article Online
View Journal | View Issue

Cite this: *Soft Matter*, 2015, **11**, 4944

Time-dependent gel to gel transformation of a peptide based supramolecular gelator†

Abhishek Baral,[a] Shibaji Basak,[a] Kingshuk Basu,[a] Ashkan Dehsorkhi,[b] Ian W. Hamley[b] and Arindam Banerjee*[a]

Received 6th April 2015,
Accepted 20th May 2015

DOI: 10.1039/c5sm00808e

www.rsc.org/softmatter

A dipeptide with a long fatty acid chain at its N-terminus gives hydrogels in phosphate buffer in the pH range 7.0–8.5. The hydrogel with a gelator concentration of 0.45% (w/v) at pH 7.46 (physiological pH) provides a very good platform to study dynamic changes within a supramolecular framework as it exhibits remarkable change in its appearance with time. Interestingly, the first formed transparent hydrogel gradually transforms into a turbid gel within 2 days. These two forms of the hydrogel have been thoroughly investigated by using small angle X-ray scattering (SAXS), powder X-ray diffraction (PXRD), field emission scanning electron microscopic (FE-SEM) and high-resolution transmission electron microscopic (HR-TEM) imaging, FT-IR and rheometric analyses. The SAXS and low angle PXRD studies substantiate different packing arrangements for the gelator molecules for these two different gel states (the freshly prepared and the aged hydrogel). Moreover, rheological studies of these two gels reveal that the aged gel is stiffer than the freshly prepared gel.

Introduction

Low molecular weight gelators[1–15] (LMWGs) remain to be an interesting topic in current research due to their attractive properties and many applications. These gels have been used for various applications in drug delivery,[16–20] tissue engineering,[21,22] oil spill recovery,[23–25] synthesis of noble metal nanoparticles/nanoclusters,[26,27] catalysis for chemical reactions[28] and others.[29–31] Among these gels, amino acid and peptide hydrogelators are attractive candidates for making functional gel based soft materials due to their excellent biocompatibility and biodegradability.[16,24,32] Supramolecular hydrogels encapsulate a large number of water molecules within their nanofibrillar network formed by the assembly of gelator molecules by using different non-covalent interactions including hydrogen bonding, π–π stacking, hydrophobic and van der Waals interactions. Unlike polymer gels, supramolecular LMWGs are held together by various non-covalent interactions, of which some of these interactions lack directionality, which triggers reversibility in the supramolecular gel network. So, there is a possibility of dynamic changes within the supramolecular gels which are responsive to external stimuli like heat, light, mechanical strength, pH, salt concentration and others.

LMWGs within a hydrogel network self-assemble in aqueous medium by maintaining a delicate balance between hydrophilicity and hydrophobicity. A typical hydrogelator molecule contains at least two parts, a hydrophilic region that interacts favorably with water molecules thus enhancing its solubility and a hydrophobic region that promotes self-assembly in water. The hydrophobic part of the molecule tends to come closer to each other for minimizing their exposure towards water (hydrophobic interaction), thus facilitating self-assembly between these molecules. On the other hand, the hydrophilic part plays a crucial role as its presence and absence provide a difference between self-assembly and precipitation respectively.[2] Thermodynamic parameters have been used to explain how small changes in molecular structure and solvent can turn gelators into non-gelators.[33–35]

The non-covalent nature of the interaction affords sufficient flexibility to the supramolecular network as supramolecular species can reversibly dissociate or associate, cut or repair through their non-covalent interactions and this gives rise to reorganized arrangement of gelators in the gel phase.[36,37] This reorganization can be initiated by the application of external stimuli like light,[38–40] pH[41,42] or enzymes.[43,44] In most cases gel-to-sol or sol-to-gel transformation has been reported,[45] while gel-to-gel transformation is relatively rare in this regard.[46–48] Thus, it will be interesting to synthesize and study a new gelator molecule that can exhibit observable gel-to-gel transformation through the naked eyes.

[a] *Department of Biological Chemistry, Indian Association for the Cultivation of Science, Jadavpur, Kolkata-700032, India. E-mail: bcab@iacs.res.in; Fax: +91 33-2473-2805*

[b] *Department of Chemistry, University of Reading, Whitenights, Reading, RG6, 6AD, UK*

† Electronic supplementary information (ESI) available: Synthetic procedure, detailed instrumentation, NMR and mass spectra, gel images, DSC themograms, FT-IR, X-ray analysis and CAC plots, absorbance plot and SAXS, WAXS and PXRD tables. See DOI: 10.1039/c5sm00808e

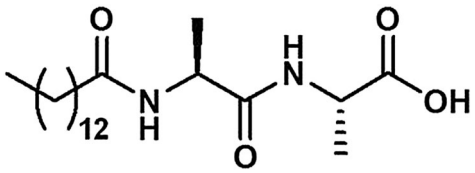

Fig. 1 Chemical structure of the gelator peptide **MAA**.

As the dynamic interchange between various non-covalent interactions is common to the self-assembled gelators, a peptide based amphiphile with a long fatty acyl chain has been chosen in such a way that the peptide bond (–CONH–) will provide hydrogen bonding functionality, the terminal fatty acyl chain will promote hydrophobic interaction and gelation[49–51] and in the other portion, the carboxylic part at the C-terminus will promote interaction with solvent (water) molecules. The long aliphatic chain located at the N-terminus is responsible for hydrophobic interaction and the smaller side chain of the alanine residues (unlike other comparatively larger amino acid residues) permits closer interaction between the hydrophobic tails of these self-assembling peptide amphiphiles with respect to time compared to other peptide amphiphiles with larger aromatic side chains. In this study, the main objective is to explore the packing arrangement among the self-assembling gelator molecules of **MAA** (Fig. 1) with respect to time and to examine whether there is a time-dependent change in the assembly pattern amongst gelators. Due to the absence of aromatic side chains or bulky aliphatic side chains (like valine, leucine), the interaction between the long alkyl chains is more efficient and they can interact with one another more strongly to impart specific arrangements in self-association and gelation compared to a peptide based amphiphilic molecule with an aromatic/bulky aliphatic group. The dipeptide **MAA** forms a hydrogel at pH 7.46 and a time-dependent gradual transformation from a transparent to turbid gel has been observed by the naked eye. Interestingly, the freshly prepared and the aged gel exhibit different packing patterns as evident from respective small angle X-ray studies. Thus, this study provides a wonderful platform to understand and gain knowledge of the time-dependent dynamic chemistry existing within the hydrogel matrix.

Experimental section

Materials and methods

Myristic acid, L-alanine and pyrene were purchased from Aldrich. HOBt, sodium dihydrogen phosphate and disodium hydrogen phosphate were purchased from Merck. DCC, NaOH, MeOH, silica gel (100–200 mesh), Et_2O, petroleum ether (60–80 °C), EtOAc and DMF were purchased from SRL (India). Details of the synthetic procedures of gelator peptide and instrumentation details are given in the ESI.†

Results and discussion

Gelation study

The myristic acid containing dipeptide **MAA** (Fig. 1) forms hydrogels in a phosphate buffer solution in the pH range 7.0–8.5. In this study, an intermediate pH 7.46 was chosen for our gelation study. For preparation of the hydrogel, the gelator was weighed in a glass vial and 1 mL of phosphate buffer was added and heated on a hot plate to make a clear solution of the peptide. The solution was then allowed to come down to room temperature to form a hydrogel. Interestingly, the visual appearance of the hydrogel is extremely sensitive towards gelator concentration. The minimum gelation concentration (MGC) was found to be 0.3% (w/v). However, a time-dependent change in the appearance of the hydrogel (transparent to turbid) was clearly observed, when the gelator concentration was in the range of 0.4–0.5% (w/v) at pH 7.46 (Fig. 2). At this concentration range, a transparent hydrogel was formed upon allowing it to stand for about 2 hours. The transparent hydrogel started to become turbid after 10 hours and a completely turbid gel was obtained after almost two days (Fig. 2). However, this gradual observable change took place rapidly at higher concentration. For example, when 6 mg of gelator was taken for preparation of a 0.6% (w/v) hydrogel, transparent–turbid transition was obtained after 60–70 minutes (Fig. S4, ESI†). On the other hand, when the concentration is lower than 0.4% (w/v), a transparent to turbid change was observed, however, in this case only a loose gel was obtained. So, a 0.45% (w/v) hydrogel of **MAA** at pH 7.46 was used for all our studies reported in this paper. Under these conditions a noticeable change can be observed through the naked eyes. These observations for the hydrogel can be beautifully exploited to gain knowledge about the ongoing dynamic self-assembly within the hydrogel matrix. There are also some earlier reports on polymorphic transitions of supramolecular gel based systems. Different morphological structures of polymorphs were obtained for oligo(*p*-phenylene-ethynylene) (OPV) based organogelators that can be controlled by varying different conditions like gelator concentration, humidity *etc.*[52] There is also a recent report on polymorphism in a peptide based hydrogelator, in which various polymorphs were observed upon modification of

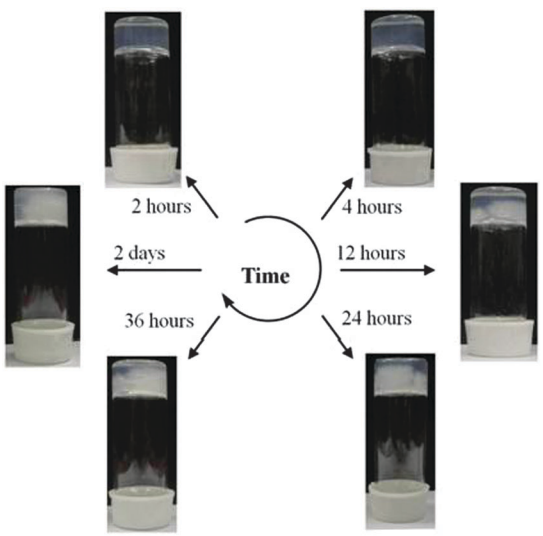

Fig. 2 Time-dependent transformation of one gel form (transparent) to another gel form (turbid) at a fixed **MAA** concentration of 4.5 mg mL^{-1} (0.45% (w/v)).

temperature, aging time and ultrasound.[53] Though our result of time-dependent phase change is somewhat similar to the previous report,[53] a smooth time-dependent transparent–turbid transition is observed in this study and this transition is not associated with any external stimuli unlike previous studies. To gain more knowledge about the phenomenon, we investigated whether this gel formation is due to the kinetic or thermodynamic effect. Thus, the gelator solution was cooled by two different methods: (i) fast cooling or directly allowing the gelator solution to cool at room temperature (around 29 °C), (ii) relatively slow cooling. So, the rate of cooling was varied. At first, 4.5 mg of the gelator was taken in a glass vial and 1 mL of phosphate buffer (pH 7.46) was added to it. The mixture was then heated to about 75 to 80 °C in a water bath to get a clear solution. Then this solution was immediately transferred to a water bath with its temperature around 29 °C. In another procedure, this hot solution was kept in a 75 °C water bath. The hot gelator solution in this case was cooled slowly with the water of the water bath, before it reached room temperature (29 °C) after about 3 hours. The solution which was kept at 29 °C produced a gel phase soft material within 2 hours, while the gelator solution which was allowed to cool slowly from 75 °C to 29 °C did not produce a gel phase material, instead a turbid viscous solution was obtained (Fig. S5, ESI†). The gel phase material obtained from procedure (i) exhibits a transparent–turbid phase transition similar to the one described above, while the viscous turbid solution remained unchanged when observed for 2 days. Thus, it may be concluded that the transparent gel formation is a kinetic effect and the formation of a turbid viscous mixture is likely to be a thermodynamic effect. This is because the fast cooling results in entrapment of a kinetically trapped gel phase material, while the slow cooling triggers fibrous turbid aggregate formation, not gelation. So, there appears to be a competition between gelation and fibrous turbid aggregate formation, depending whether the cooling procedure is fast or slow. These studies indicate that the **MAA** hydrogelator exhibits a dynamic phase transformation that depends on time, gelator concentration as well as on the rate of cooling of the hot gelator solution.

Dynamic Scanning Calorimetry (DSC) of both the freshly prepared and the aged hydrogels was carried out to examine the thermo-reversibility as well as to probe whether there is any change in the DSC thermograms for two different phase gels (Fig. S6, ESI†). It was observed that an endotherm for the fresh gel was obtained at 52.0 °C and for the aged gel it was 52.9 °C upon heating, and an exotherm for these two gels was observed at 31.9 °C and 33 °C upon cooling for the fresh and the aged gel respectively. This indicates that there is a small difference for these two gel phases in both endotherm and exotherm. However, these thermograms showed sharp peaks for the aged gel, while weaker and broader peaks were found for the freshly prepared gel. So, it can be concluded that the phase transition for the aged gel is more prominent from that of the fresh gel. This can be due to the fact that stiffness of the gel is more for the aged gel than that of the freshly prepared gel. This happens due to the more ordered packing arrangement of these gelator molecules within the aged gel compared to that of the freshly prepared gel.

Morphology

It is interesting to explore the morphological behavior of the hydrogel with respect to time and to examine whether there is a time-dependent change of the morphological features of the hydrogel. Thus, electronic microscopic studies were conducted to observe not only the morphological features of the hydrogel but also to examine, whether there is any difference between the freshly prepared and the aged gel microscopically. Field emission scanning electron microscopic (FE-SEM) (Fig. 3) and high resolution transmission electron microscopic (HR-TEM) studies (Fig. 4) were carried out with the respective xerogels obtained from the freshly prepared gel as well as from the aged gel. Both SEM and TEM images obtained from the freshly prepared and the aged gel suggest the formation of a nanofibrillar network structure responsible for gelation. Interestingly, these gel fibres display helicity within the three-dimensional network structure. However, the pitch length of these helical fibres are changing with respect to time as evident from the respective SEM and TEM images of the freshly prepared gel and the aged gel (Fig. 3 and 4). The TEM image of the freshly prepared gel (Fig. 4a and Fig. S7a, ESI†) indicates that some of these gel nanofibers are helical in nature and the helicity of the nanofiber is not uniform, which means that the pitch length along a single nanofiber is not fixed which are indicated by the yellow arrows in Fig. 4a. However, TEM images (Fig. 4b and Fig. S7b, ESI†) of the aged gel indicate that there is uniformity in the pitch length of the helical nanofibers as the pitch length of a particular nanofiber obtained from two days aged gel is constant as marked by the yellow arrows in Fig. 4b.

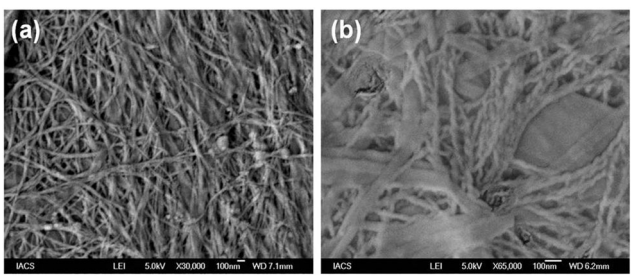

Fig. 3 The FE-SEM image indicates twisted fibers for the (a) freshly prepared and the (b) aged **MAA** xerogel.

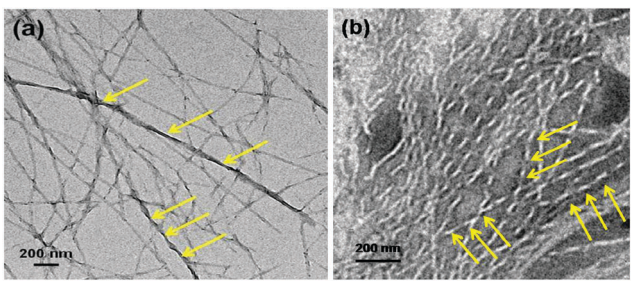

Fig. 4 HR-TEM image of the (a) freshly prepared xerogel. The arrows show different pitch lengths for different nanofibers. The arrows also demonstrate the non-uniformity of the pitch of fibres. (b) HR-TEM image of the aged xerogel. The three equidistant arrows show uniformity in the pitch length for the nanofiber.

The pitch lengths observed from the TEM images are 90–110 nm for the aged gel nanofibers. On the other hand, the helical fibers of the freshly prepared gel possess much higher pitch lengths than the two days aged gel nanofiber (in some fibres it is as high as 450 nm). So, it can be stated that fibres of the aged gel possess much regular and prominent twisting than that of the freshly prepared hydrogel. All these outcomes indicate that a more ordered network of gelator molecules may lead to uniform twisting of the fibres with time and it highlights a time-dependent dynamic change within the microscopic environment of the gel.

FT-IR studies

Fourier transform infra red (FT-IR) studies of these xerogels (Fig. 5) were carried out to know more about interactions involved amongst the gelator molecules. It is also interesting to see whether there is any change in the FT-IR spectra upon aging of the hydrogel. In the xerogel obtained from the freshly prepared hydrogel, significant peaks were observed at 3311 cm^{-1}, 1631 cm^{-1} and 1549 cm^{-1} corresponding to the hydrogen-bonded N–H stretching, C=O stretching (amide I) and N–H bending (amide II) respectively.[19] On the other hand, the corresponding peaks were found at 3299 cm^{-1}, 1635 cm^{-1} and 1547 cm^{-1} for the xerogel obtained from the aged gel. The shifting of the N–H stretching band towards lower frequency upon aging of the hydrogel indicates a more ordered hydrogen bonded network structure in the aged gel state.

Kinetics of the transformation from the freshly prepared to the aged gel was also determined with a D_2O solution of the gelator using FT-IR study (Fig. S8, ESI†). Two prominent peaks were observed at 1628 cm^{-1} and 1709 cm^{-1} for the wet gel. The peak at 1628 cm^{-1} indicates the hydrogen bonded carbonyl stretching band of the amide bond, while the peak at 1709 cm^{-1} arises from the C=O stretching frequency of the myristyl amide bond.[54] The amide carbonyl stretching peaks at 1628 cm^{-1} in the wet gel state along with the peaks at 1631 cm^{-1} and 1635 cm^{-1} from the xerogel state point towards a β-sheet-like arrangement among the gelator molecules.[54] However, in the wet gel state, FT-IR study does not signify any appreciable changes in the two major peaks with time.

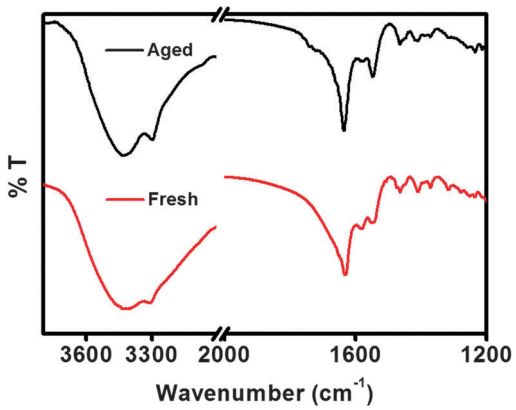

Fig. 5 FT-IR analyses of the freshly prepared and the aged gel.

SAXS, WAXS and powder XRD

The gradual change in the appearance of the hydrogel inspired us to look into the detailed packing pattern of the gelator molecules within the hydrogel. To explore, if there is any dynamic process responsible for this apparent gel-to-gel transformation, small angle X-ray scattering (SAXS) of the wet hydrogel (Fig. 6) and low angle powder XRD of the xerogel were carried out separately for the freshly prepared and the aged gel (Fig. 7). Two peaks were obtained in the SAXS experiment for the freshly prepared gel at 41.3 Å (q = 1.53 nm^{-1}) and 31.1 Å (q = 2.02 nm^{-1}) and the aged gel exhibited two sharp peaks at 42.4 Å (q = 1.48 nm^{-1}) and 32.9 Å (q = 1.91 nm^{-1}). These peaks are almost at the same position for both freshly prepared and aged gels. However, the peaks in the freshly prepared gel are broad and peaks obtained from the two days aged gel are sharp and well resolved. The appearance of sharper peaks in SAXS for the aged hydrogel indicates that a structural change has taken place with time. After that, we have performed the powder X-ray diffraction (PXRD) study in the xerogel state for these gels (freshly prepared and aged). In the aged gel two peaks were obtained at 40.48 Å (2θ = 2.18°) and 32.8 Å (2θ = 2.69°), while the freshly prepared gel contains only one peak at 32.09 Å (2θ = 2.75°). These two peaks for the aged gel (at 40.48 Å and 32.8 Å) almost match with the peaks obtained from the SAXS experiment. For the freshly prepared gel, though the 32.8 Å peak matched well with the 31.1 Å peak in the SAXS data, the other peak (at 40.4 Å) was absent in the xerogel obtained from the freshly prepared gel. So, it can be proposed that the 40.4 Å peak observed in SAXS for the freshly prepared gel is due to the aging that occurs during the experimental time. This can happen, as the recording of SAXS data requires about 6 hours. It is apparent from Fig. 2 that the aging of the gel takes much more than 6 hours.

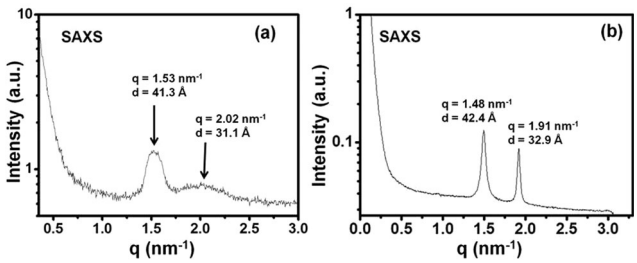

Fig. 6 The SAXS data obtained from (a) the freshly prepared/transparent hydrogel and the (b) aged/turbid hydrogel.

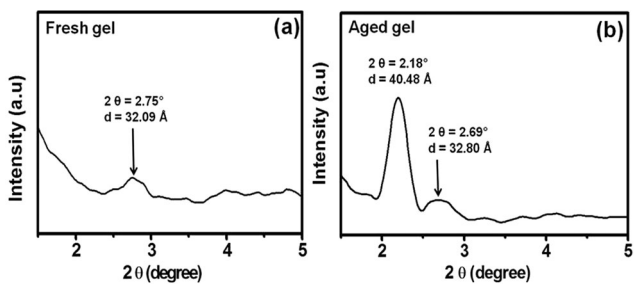

Fig. 7 The low angle powder XRD of the xerogel obtained from (a) the freshly prepared xerogel and the (b) aged/turbid xerogel.

Here, gel pictures were taken at a concentration of 4.5 mg mL^{-1} (0.45% (w/v)), while the SAXS pattern was recorded at a concentration of 6 mg mL^{-1}. This is because 4.5 mg mL^{-1} concentration is too low for the hydrogel to diffract in SAXS. On the other hand the vial pictures were taken at lower concentration (4.5 mg mL^{-1}) to observe the gradual change in gel appearance for days. As more concentration of the gelator causes faster transformation from the transparent to opaque gel state, higher concentration of the gelator in SAXS causes faster aging. So, from the low angle data it can be concluded that there is an obvious transformation from one gel phase to the other gel phase that has a more ordered structure of gelator molecules than the freshly prepared gel state. The presence of one peak at almost the same position (around 32 Å) in the low angle data (for both fresh and aged gels) and evolution of a new peak in the aged gel (around 42 Å) suggests the formation of a new interdigitated supramolecular structure with time. Thus, it can be proposed that there is a co-existence of different degrees of interdigitated structure within the self-assembled supramolecular network for the aged hydrogel.[55] To obtain further knowledge about the molecular arrangement in the supramolecular network structure, WAXS of the wet aged hydrogel (Fig. S9, ESI†) and wide angle PXRD (Fig. S10, ESI†) of the aged xerogel were performed. In WAXS, periodic peaks were observed at 7.81 Å (q = 8.04 nm^{-1}), 6.5 Å (q = 9.66 nm^{-1}) and 5.45 Å (q = 11.52 nm^{-1}) (these peaks are listed in Table S1, ESI†). Significant peaks were also observed in wide angle PXRD at d values of 10.29 Å ($2\theta = 8.58^{\circ}$), 7.82 Å ($2\theta = 11.36^{\circ}$), 6.96 Å ($2\theta = 12.7^{\circ}$), 5.37 Å ($2\theta = 16.47^{\circ}$) and 5.22 Å ($2\theta = 16.9^{\circ}$) (the peaks are listed in Table S2, ESI†). Interestingly, some of the d values for both experiments match with each other, although some peaks are missing in the WAXS data due to strong scattering from water molecules. Peaks corresponding to the d spacing of 4.92 Å (q = 12.78 nm^{-1}) and 4.75 Å (q = 13.22 nm^{-1}) may arise from the β-strand spacing oriented at different azimuthal angles.[54] Thus, there is a co-existence of interdigitated structures as well as β-sheet-like structures within the supramolecular matrix for the aged gel.[54]

Rheology

X-ray scattering and FT-IR studies give enough hints to believe that better hydrogen bonding occurs with aging that results in a more ordered packing between these gelator molecules within the aged hydrogel. So, it may lead to some changes in the strength of the hydrogel upon aging. To reinforce this point rheological investigations can be a wonderful tool. This drives us to carry out a frequency sweep experiment (Fig. 8a) of both the freshly prepared and the aged gel. It reveals an almost five fold increase in the storage modulus value (G') with aging of the hydrogel, when the experiment is done in the angular frequency range 5–100 rad s^{-1}. This gives an indication of increase in gel stiffness upon aging. However $\tan\delta(G''/G')$ for both aged and freshly prepared gels are somewhat similar and there is no much difference in $\tan\delta$ values of freshly prepared and aged gels. The oscillatory stress sweep experiment (Fig. 8b) shows that almost similar yield stress (53 Pa) is required to break the freshly prepared gel as well as the aged gel. So, it can be said that there is no appreciable difference in the mechanical strength for the aged gel and the freshly prepared gel.

Fluorescence and absorption studies

We are much interested to monitor any time-dependent change occurring within the gel phase material that can be the reason for transparent-to-opaque transition of the hydrogel. The local polarity change within an aggregated system can be best scrutinized with a fluorescent probe like pyrene.[56–58] This is because the fluorescence spectrum of pyrene is much sensitive to the environment in its vicinity. The non-planer excited state of pyrene has different structural features than its planar ground state and this is the reason for its sensitiveness towards its neighborhood. A concentration dependent study with the gelator solution is helpful to determine the critical aggregation concentration (CAC) of a particular aggregated solution.[58] For determining the CAC, ten different solutions of the gelator in buffer were taken and the same amount of methanol solution of pyrene (with same concentration of pyrene) was added to it. Fluorescence of these solutions was noted and an I_3/I_1 *vs.* concentration plot gives critical aggregation concentration (CAC) of the hydrogelator at 0.025% (w/v) as after this point, I_3/I_1 values almost increase linearly with an increase in concentration (Fig. S11, ESI†). Interestingly, there is a sudden drop in the I_3/I_1 value as we go from

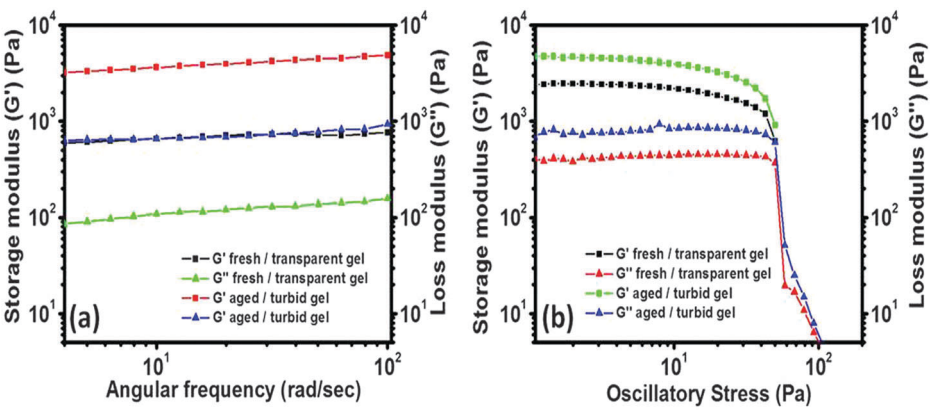

Fig. 8 (a) Frequency and (b) stress sweep rheological analyses of the **MAA** hydrogel. The stress sweep expt shows yield stress of both aged and freshly prepared gels to be at 53 Pa.

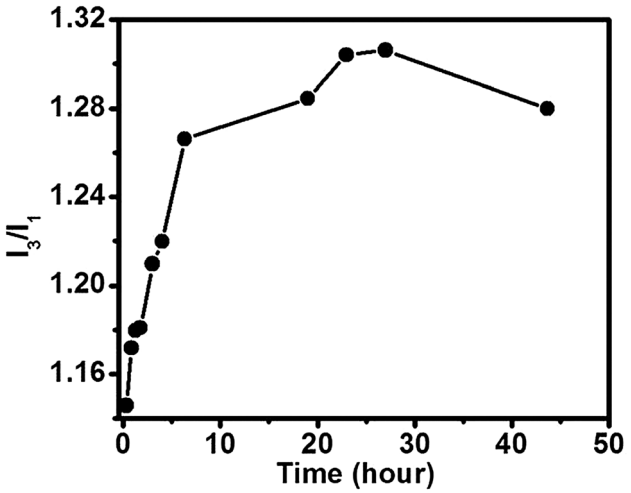

Fig. 9 Change in the of I_3/I_1 ratio of pyrene fluorescence as a function of time with the gelator **MAA** (4.5 mg mL^{-1}) at 25 °C.

0.1% (w/v) to 0.2% (w/v). This is because the gelator **MAA** forms gel at 0.2% (w/v). Thus, the second inflection point at 0.1% (w/v) (after the CAC point at 0.025% (w/v)) is close to the critical gelation concentration of **MAA**.[58] To study the time-dependent change, a small amount of a dilute methanol solution of pyrene was added to the hydrogel (0.45% (w/v)) and the fluorescence emission spectrum of the pyrene containing hydrogel was recorded time to time. The ratio of the two vibronic bands (I_3/I_1) is plotted with time (Fig. 9). A steady rise of the I_3/I_1 values is observed up to a few hours of gel formation but after about 9 hours the line corresponding to the I_3/I_1 values almost becomes parallel to the *x*-axis. This indicates that a reorganization process is working for almost 9 hours between the gelator molecules and this results in a transparent to turbid gel transition. Thereafter a steady-state is regained and no major change in the I_3/I_1 values is observed. The sharp enhancement in the I_3/I_1 values with time is an indication that the pyrene molecules are enjoying an increasing hydrophobic environment within the gel matrix.[57] These gelator molecules along with the solvent molecules afford a supramolecular platform that increases its hydrophobicity with time before reaching an equilibrium state. So, it can be concluded that the hydrophobic environment for the freshly prepared gel state and the aged gel state is significantly different from that of the aged gel state. The transparent-to-turbid visual change in the hydrogel can be measured through a UV absorption study as turbidity change can be monitored from the variation in transmitted light.[59] Thus, a small amount of water solution of Rhodamine B was added to 1 mL of 0.45% (w/v) hydrogel and time to time absorbance values at 553 nm (λ_{max} of reference dye Rhodamine B) were noted (Fig. S12, ESI†). It was found that the absorbance values gradually increased (decrease in light transmittance) with time before reaching a constant value after almost 8 hours. This suggests that after 8 hours, a steady state is obtained with no appreciable change in the absorbance value. In other words, it can be stated that the transparent to turbid gel-state transformation is almost completed after about 8 hours. The absorption study with a more concentrated hydrogel (0.6% (w/v)) exhibits very fast transparent-turbid transition. Thus, the UV study provides an *in situ* and quantitative measurement to track the aging process

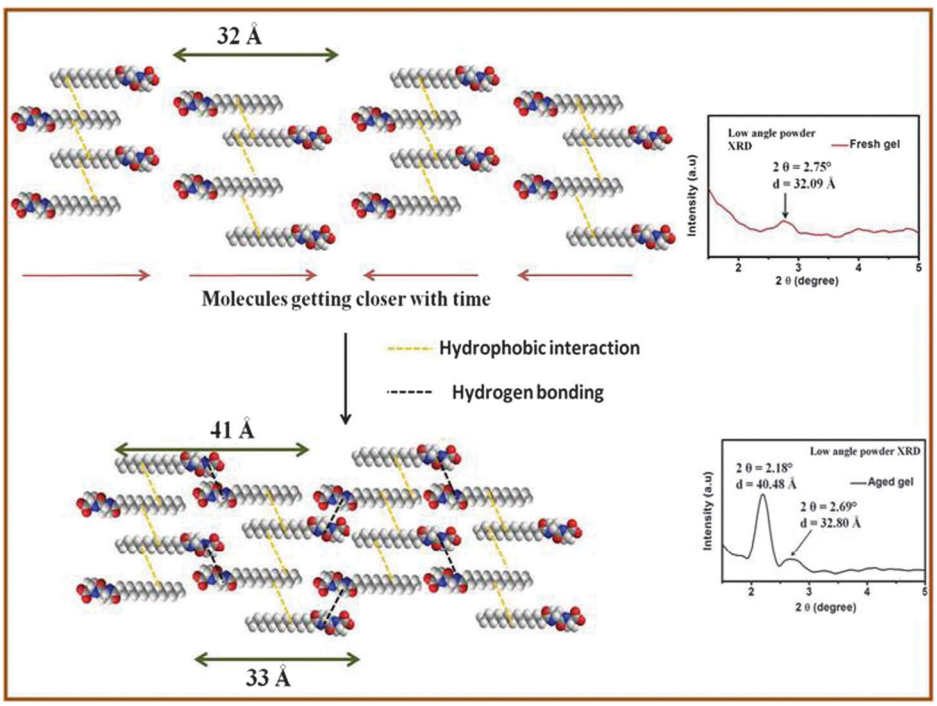

Fig. 10 Proposed schematic models for the packing arrangements of gelator molecules based on the small angle X-ray studies of the freshly prepared gel and the aged (2 days) gel. This indicates a possible mode of intermolecular packing arrangement by which the gelator **MAA** molecules get closely packed with the progress of time.

occurring within the hydrogel. Furthermore, this study along with the time-dependent fluorescence study with pyrene suggests that the increase in turbidity and enhancement of the hydrophobic environment within the gel matrix goes hand in hand.

The physical appearance, morphological studies, SAXS, PXRD obtained from the xerogels of **MAA** and time-dependent pyrene binding study of the hydrogel suggest that the hydrogels in two different gel phases (freshly prepared and aged) are distinctly different from each other. Previous reports of gel-to-gel transformation have shown that either this is triggered by heat,[47] formation of gel at different gel temperatures[46] or ultrasound.[48] However, phase transformation in the gel state obtained from a peptide based hydrogelator where aging time is the only determining factor is rare.[59] This is a unique example of time-dependent gel-to-gel transformation of an amphiphilic hydrogelator maintaining the same concentration, pH, solvent system and temperature. Moreover, the *in situ* changes like change in the packing pattern of the gelator molecules and enhanced uniformity in the nanofibres are reflected through a naked eye observable change. Based on our observations mainly from the SAXS of the fresh and aged hydrogels and powder XRD data of the xerogel obtained from the fresh and aged hydrogels, a schematic model for the packing arrangement has been proposed (Fig. 10).

Conclusion

This is a nice demonstration of a peptide based hydrogel that transforms into another gel form with the progress of time and is evident through small angle X-ray scattering, powder X-ray diffraction and HR-TEM analysis. The arrangement of gelator molecules is different in these two different gel states. Compaction of the packing arrangement of gelator molecules occurs upon aging as evident from small angle X-ray analysis and electron microscopic analysis. This is an interesting example of a time-dependent change in the supramolecular assembly of the same gelator molecule in the same solvent environment that brings about a visible macroscopic appearance of the gel from the transparent gel state to the turbid gel state upon aging.

Acknowledgements

A.B. and K.B. gratefully acknowledge CSIR, New Delhi (India), and S.B. acknowledges IACS for financial assistance. A. Banerjee and Ian W. Hamley gratefully acknowledge DST-UKIERI bilateral project (project no. DST/INT/UK/P-64/2014). We acknowledge Dr. Daniel Hermida-Merino at the ESRF, Grenoble for WAXS measurements.

Notes and references

1 R. G. Weiss, *J. Am. Chem. Soc.*, 2014, **136**, 7519–7530.
2 J. Raeburn, A. Z. Cardoso and D. J. Adams, *Chem. Soc. Rev.*, 2013, **42**, 5143–5156.
3 X. Du, J. Zhou and B. Xu, *Chem. – Asian J.*, 2014, **9**, 1446–1472.
4 S. S. Babu, V. K. Praveen and A. Ajayaghosh, *Chem. Rev.*, 2014, **114**, 1973–2129; S. S. Babu, V. K. Praveen, K. K. Kartha, S. Mahesh and A. Ajayaghosh, *Chem. – Asian J.*, 2014, **9**, 1830–1840.
5 N. Javid, S. Roy, M. Zelzer, Z. Yang, J. Sefcik and R. V. Ulijn, *Biomacromolecules*, 2013, **14**, 4368–4376.
6 S. Banerjee, R. K. Das, P. Terech, A. d. Geyer, C. Aymonier, A. Loppinet-Serani, G. Raffy, U. Maitra, A. D. Guerzo and J.-P. Desvergne, *J. Mater. Chem. C*, 2013, **1**, 3305–3316.
7 S. K. Samanta and S. Bhattacharya, *J. Mater. Chem.*, 2012, **22**, 25277–25287.
8 S. Bhattacharya and S. K. Samanta, *Langmuir*, 2009, **25**, 8378–8381.
9 K. Liu and J. W. Steed, *Soft Matter*, 2013, **9**, 11699–11705.
10 J. A. Foster, R. M. Edkins, G. J. Cameron, N. Colgin, K. Fucke, S. Ridgeway, A. G. Crawford, T. B. Marder, A. Beeby, S. L. Cobb and J. W. Steed, *Chem. – Eur. J.*, 2014, **20**, 279–291.
11 W. Edwards and D. K. Smith, *J. Am. Chem. Soc.*, 2014, **136**, 1116–1124.
12 W. Edwards and D. K. Smith, *J. Am. Chem. Soc.*, 2013, **135**, 5911–5920.
13 A. Z. Cardoso, A. E. A. Alvarez, B. N. Cattoz, P. C. Griffiths, S. M. King, W. J. Frith and D. J. Adams, *Faraday Discuss.*, 2013, **166**, 101–116.
14 V. Castelletto, R. J. Gouveia, C. J. Connon, I. W. Hamley, J. Seitsonen, J. Ruokolainen, E. Longo and G. Siligardi, *Biomater. Sci.*, 2014, **2**, 867–874.
15 J. Nanda, A. Biswas and A. Banerjee, *Soft Matter*, 2013, **9**, 4198–4208.
16 J. Li, X. Li, Y. Kuang, Y. Gao, X. Du, J. Shi and B. Xu, *Adv. Healthcare Mater.*, 2013, **2**, 1586–1590.
17 J. Naskar, G. Palui and A. Banerjee, *J. Phys. Chem. B*, 2009, **113**, 11787–11792.
18 J. Nanda and A. Banerjee, *Soft Matter*, 2012, **8**, 3380–3386.
19 A. Baral, S. Roy, A. Dehsorkhi, I. W. Hamley, S. Mohapatra, S. Ghosh and A. Banerjee, *Langmuir*, 2014, **30**, 929–936.
20 C. Yan, M. E. Mackay, K. Czymmek, R. P. Nagarkar, J. P. Schneider and D. J. Pochan, *Langmuir*, 2012, **28**, 6076–6087.
21 L. A. Haines, K. Rajagopal, B. Ozbas, D. A. Salick, D. J. Pochan and J. P. Schneider, *J. Am. Chem. Soc.*, 2005, **127**, 17025–17029.
22 K. M. Galler, L. Aulisa, K. R. Regan, R. N. D'Souza and J. D. Hartgerink, *J. Am. Chem. Soc.*, 2010, **132**, 3217–3223.
23 S. R. Jadhav, P. K. Vemula, R. Kumar, S. R. Raghavan and G. John, *Angew. Chem., Int. Ed.*, 2010, **49**, 7695–7698.
24 S. Basak, J. Nanda and A. Banerjee, *J. Mater. Chem.*, 2012, **22**, 11658–11664.
25 Rajkamal, D. Chatterjee, A. Paul, S. Banerjee and S. Yadav, *Chem. Commun.*, 2014, **50**, 12131–12134.
26 J. Nanda, A. Biswas, B. Adhikari and A. Banerjee, *Angew. Chem., Int. Ed.*, 2013, **52**, 5041–5045.
27 S. Roy and A. Banerjee, *Soft Matter*, 2011, **7**, 5300–5308.
28 F. Rodríguez-Llansola, J. F. Miravet and B. Escuder, *Chem. Commun.*, 2009, 7303–7305.

29 A. Wada, S. Tamaru, M. Ikeda and I. Hamachi, *J. Am. Chem. Soc.*, 2009, **131**, 5321–5330.
30 G. John, B. V. Shankar, S. R. Jadhav and P. K. Vemula, *Langmuir*, 2010, **26**, 17843–17851.
31 D. Kühbeck, G. Saidulu, K. R. Reddy and D. D. Díaz, *Green Chem.*, 2012, **14**, 378–392.
32 S. Basak, N. Nandi and A. Banerjee, *Chem. Commun.*, 2014, **50**, 6917–6919.
33 M. L. Muro-Small, J. Chen and A. J. McNeil, *Langmuir*, 2011, **27**, 13248–13253.
34 I. Giannicchi, B. Jouvelet, B. Isare, M. Linares, A. D. Cort and L. Bouteiller, *Chem. Commun.*, 2014, **50**, 611–613.
35 J. Świergiel, L. Bouteiller and J. Jadżyn, *Soft Matter*, 2014, **10**, 8457–8463.
36 J.-M. Lehn, *Chem. Soc. Rev.*, 2007, **36**, 151–160.
37 P. Cordier, F. Tournilhac, C. Soulié-Ziakovic and L. Leibler, *Nature*, 2008, **451**, 977–980.
38 S. Yagai and A. Kitamura, *Chem. Soc. Rev.*, 2008, **37**, 1520–1529.
39 J. Raeburn, T. O. McDonald and D. J. Adams, *Chem. Commun.*, 2012, **48**, 9355–9357.
40 Y. Wu, S. Wu, G. Zou and Q. Zhang, *Soft Matter*, 2011, **7**, 9177–9183.
41 D. M. Wood, B. W. Greenland, A. L. Acton, F. Rodríguez-Llansola, C. A. Murray, C. J. Cardin, J. F. Miravet, B. Escuder, I. W. Hamley and W. Hayes, *Chem. – Eur. J.*, 2012, **18**, 2692–2699.
42 R. J. Mart, R. D. Osborne, M. M. Stevens and R. V. Ulijn, *Soft Matter*, 2006, **2**, 822–835.
43 S. Toledano, R. J. Williams, V. Jayawarna and R. V. Ulijn, *J. Am. Chem. Soc.*, 2006, **128**, 1070–1071.
44 G. Chen, C. Ren, L. Wang, B. Xu and Z. Yang, *Chin. J. Chem.*, 2012, **30**, 53–58.
45 T. Kato, Y. Hirai, S. Nakaso and M. Moriyama, *Chem. Soc. Rev.*, 2007, **36**, 1857–1867.
46 A. Kotlewski, B. Norder, W. F. Jager, S. J. Picken and E. Mendes, *Soft Matter*, 2009, **5**, 4905–4913.
47 V. A. Mallia, P. D. Butler, B. Sarkar, K. T. Holman and R. G. Weiss, *J. Am. Chem. Soc.*, 2011, **133**, 15045–15054.
48 X. Yu, Q. Liu, J. Wu, M. Zhang, X. Cao, S. Zhang, Q. Wang, L. Chen and T. Yi, *Chem. – Eur. J.*, 2010, **16**, 9099–9106.
49 A. Dehsorkhi, V. Castelletto and I. W. Hamley, *J. Pept. Sci.*, 2014, **20**, 453–467.
50 Y. Fu, B. Li, Z. Huang, Y. Li and Y. Yang, *Langmuir*, 2013, **29**, 6013–6017.
51 C. Berdugo, J. F. Miravet and B. Escuder, *Chem. Commun.*, 2013, **49**, 10608–10610.
52 A. Gopal, R. Varghese and A. Ajayaghosh, *Chem. – Asian J.*, 2012, **7**, 2061–2067.
53 S. Díaz-Oltra, C. Berdugo, J. F. Miravet and B. Escuder, *New J. Chem.*, 2015, **39**, 3785–3791.
54 V. Castelletto, R. M. Gouveia, C. J. Connon and I. W. Hamley, *Faraday Discuss.*, 2013, **166**, 381–397.
55 V. Castelletto, G. Cheng, C. Stain, C. J. Connon and I. W. Hamley, *Langmuir*, 2012, **28**, 11599–11608.
56 K. Kalyanasundaram and J. K. Thomas, *J. Am. Chem. Soc.*, 1977, **99**, 2039–2044.
57 J. Aguiar, P. Carpena, J. A. Molina-Bolívar and C. C. Ruiz, *J. Colloid Interface Sci.*, 2003, **258**, 116–122.
58 S. Mukhopadhyay, U. Maitra, Ira, G. Krishnamoorthy, J. Schmidt and Y. Talmon, *J. Am. Chem. Soc.*, 2004, **126**, 15905–15914.
59 E. R. Draper, T. O. McDonald and D. J. Adams, *Chem. Commun.*, 2015, **51**, 6595–6597.